Chaos in long Josephson junctions without external rf driving force

W. J. Yeh,* O. G. Symko, and D. J. Zheng
Department of Physics, University of Utah, Salt Lake City, Utah 84112
(Received 6 October 1989)

Simulations of long Josephson junctions in an external magnetic field show a variety of chaotic behaviors. They consist of period-doubling bifurcation, intermittency between and within Fiske steps, and quasiperiodic motion at Fiske steps. A physical explanation for the chaotic behavior is presented. The influence of surface resistance to the chaotic motion is investigated. A diagram in terms of dissipation and magnetic field is constructed to show where chaos occurs for a long junction.

I. INTRODUCTION

In recent years, long Josephson junctions have attracted attention because of the variety of fundamental superconductivity phenomena they display and because they can be used in high-speed applications. Such junctions support fluxon (quantized vortex) motion, which causes current steps in the I-V curves, a well-established phenomenon. Various sorts of fluxon motions and fluxon interactions have been found theoretically and experimentally.[1-7] It turns out that a long Josephson junction also provides a very good system for studying instabilities in time and space-time.[8] In a driven damped sine-Gordon equation, which is the model for long Josephson junctions, chaotic behavior has been found under the influence of spatially uniform or nonuniform oscillating driving forces.[8-11] However, from the application point of view, most devices using long Josephson junctions are biased in a constant external magnetic field without an external rf driving force.[12-14] It is of importance to investigate the chaotic behavior in this situation as it has not been fully studied; this is the objective of this paper. Other groups working on this subject[15,16] have found intermittency chaos in perturbed sine-Gordon models in a constant magnetic field and for a specific set of parameters. Our goal is to investigate in more detail chaotic behavior in long junctions.

Recently we presented[17] experimental data and simulation results which showed the existence of chaos in long Josephson junctions. As an extension of that work, we present here detailed simulation results of chaotic behavior in long Josephson junctions modeled by the perturbed sine-Gordon equation in constant magnetic fields. From our numerical calculations we show that, in addition to intermittent chaos (which is often encountered in simulations), the route of period-doubling bifurcations leading to chaos can be located.[18] This result demonstrates unambiguously that chaotic motion indeed exists in our system and that for multidimensional systems chaos is really low dimensional. Also, we find that in specific regions quasiperiodic motion can be found.

Following the Introduction, the paper is organized as follows. In Sec. II the mathematical model for a long junction is described and the boundary conditions for the calculations are presented. In Sec. III a simple argument is given for the existence of the chaotic behavior in our system. In Sec. IV wave forms at a few Fiske steps (FS's) are presented along with the nonperiodic behavior. In Sec. V a brief survey of chaos relevant to our experiments is given so that it can be avoided when using real long junctions in applications. Section VI deals with the surface impedance term and its relevance to chaotic motion. The last section deals with a discussion of our simulations and their relevance to practical systems.

II. MODELING OF A LONG JOSEPHSON JUNCTION

The one-dimensional long Josephson junction is modeled by the perturbed sine-Gordon equation

$$\phi_{xx}-\phi_{tt}-\sin\phi=\alpha\phi_t-\beta\phi_{xxt}-\nu\ , \tag{1a}$$

where ϕ is the usual Josephson phase variable; x is the distance along the junction normalized to the Josephson penetration length

$$\lambda_J=(\phi_0/2\pi\mu_0 d j_0)^{1/2}\ ;$$

t is the time normalized to the inverse of the Josephson plasma frequency

$$\omega_0=(2\pi j_0/\phi_0 C)^{1/2}\ ,$$

the flux quantum is ϕ_0; j_0 is the Josephson critical current density; d is the magnetic thickness of the junctions; C is the junction capacitance per unit area; α is the normalized shunt conductance per unit area that takes into account tunneling dissipation due to normal electrons; β is the normalized real part of the superconducting surface impedance which represents the surface dissipation of the moving fluxons; and ν is the dc bias current density normalized to j_0. Partial derivatives are taken with respect to x and t. Conditions corresponding to the presence of the external magnetic field which is perpendicular to the length of the junction and parallel to the plane of the barrier can be modeled by the following boundary conditions:[19]

$$\phi_x(0,t)+\beta\phi_{xt}(0,t)=\phi_x(L,t)+\beta\phi_{xt}(L,t)=\eta\ , \tag{1b}$$

where $\eta = H_{ext}/\lambda_J j_0$ is a normalized measure of the external magnetic field H_{ext}, and L is the total length of the junction normalized to λ_J. Equations (1) were integrated using an implicit finite-difference method.[20]

From Eqs. (1), apparently, there are four parameters α, β, ν, and η which govern the dynamic behavior of the long Josephson junction. In most cases of our calculations β was set to zero for simplicity. The influence of β on the chaotic behavior will be briefly discussed in Sec. VI. In our search for chaos α is varied from 0.1 to 0.4, and η spans from 0.5 to 2, which corresponds to the most practical range of the external field. The bias current ν is increased from zero to a specific current value. Besides the four explicit parameters which influence the dynamics of fluxons, there are two implicit conditions which could change the dynamics. One parameter is the length of the junction. We use the case of $L = 5$ for all the calculations presented here, as it corresponds closely to junctions that we use in applications. Another is the initial condition; different initial conditions could lead to quite different behaviors in the motion of fluxons (solitons) for the perturbed sine-Gordon equation.[21] In zero magnetic field, the number of fluxons moving in the long Josephson junction is fully determined by the initial condition when the system is in the resonant mode. However, as the system is in a magnetic field, this field plus that due to the dc bias current can generate fluxons from one end of the junction. In this sense, the initial condition is less important in our situation than in zero magnetic field. For simplicity, throughout the whole simulation, the one-fluxon initial condition is used. It is defined as

$$\phi(x,0) = F(x,0) + \sin^{-1}\nu \,, \tag{2a}$$

$$\phi_t(x,0) = F_t(x,0) \,, \tag{2b}$$

where

$$F(x,t) = 4\tan^{-1}\{\exp[(x - 2.5 + ut)/1 - u^2)^{1/2}]\} \,. \tag{2c}$$

The speed u is taken as 0.8 in the calculation. For any given set of parameters, the initial condition shown above is only used at small values of ν. As soon as a finite voltage is established along the junction, which means that the dc driving current is large enough to support the motion of fluxons, conditions at the previously calculated nearby point are taken as the initial conditions for the next point. In our calculation ν is always increased except where stated.

In this study, four kinds of plots are used as the diagnostic tools to analyze various kinds of motion in the system. The first is three-dimensional evolutions of $\phi_x(x,t)$, which can demonstrate soliton motion in the junction. The second is wave forms of $\phi_t(0,t)$, and the third is power spectra of $\phi_t(0,t)$. These two are the main tools to identify chaotic motions. The last type of plot is one of ν versus $\langle \phi_t(0,t) \rangle$ curves which corresponds to I-V curves in experimental situations, where $\langle\ \rangle$ denotes the average over a long period of time.

III. DESCRIPTION OF MODEL

There are three general conditions for the occurrence of deterministic chaos in a system. First, the system should be nonlinear. Second, there should be some dissipation in the system (chaos also occurs in nondissipative systems, but they belong to another category). Third, the dimensions of the system should be equal to or greater than three.

Our system satisfies the above three conditions and hence chaos can occur. Beyond the general statement, we will present simple arguments which will provide the physical reasons why chaotic motion should occur in our system.

Consider the boundary conditions of our system. The junction has $L > \lambda_J$, and a uniform bias current is passed through the junction which is of the overlap type. In an external magnetic field Fig. 1 represents the boundary conditions[22] which consist of two virtual fluxons sitting just outside the junction. As soon as the energy requirement for the creation of a fluxon is satisfied, one virtual fluxon will enter the junction and move in the direction such that its motion is aided by the bias current. At first let us assume that the long Josephson junction is semi-infinite. When a fluxon moves in a junction it will not be reflected back from the boundary and we will not consider the resonance of the system. If the bias current is in the right direction and it is large enough, virtual fluxons can move into the system one by one. Such a situation is just like the flux-flow state in which an array of fluxons is moving through the junction. The Josephson frequency in this situation is just a measure of how many fluxons are moving per second into the system. This Josephson frequency can be varied continuously by changing the bias current or the external magnetic field perpendicular to the junction current flow.

When the finite length of the junction is taken into account, the situation changes dramatically. Although the mechanism described above still exists, resonant frequencies appear; they are determined by the speed of the fluxons in the system and the length of the junction. Fluxons in the junction will then move in one of the modes that the system allows, i.e., standing waves will be set up; and such motion corresponds to Fiske steps which are discontinuous in frequency and which show up as current steps in the I-V curve.

Because there are two frequencies involved, one tuned continuously imposed by the bias and external field and the other one discontinuous (imposed by the junction

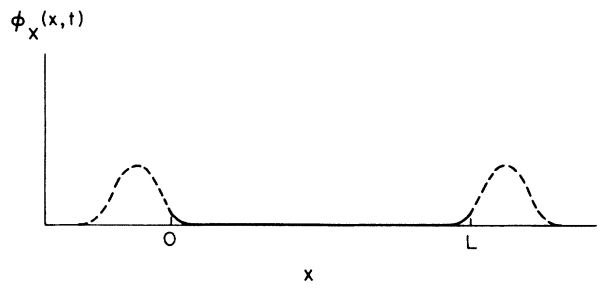

FIG. 1. The schematic representation of boundary conditions.

cavity), the appearance of chaotic motion is not surprising; the two frequencies beat against each other. Although this is one possible reason for the appearance of chaotic motion, other reasons exist as expected since the system is really a complicated one. For example, a given Fiske step can have a variety of modes[5] which are allowed to exist in the system. The interaction between modes can also give rise to nonperiodic behavior. We will discuss these possibilities in the next section.

IV. CHAOTIC BEHAVIORS

In this section various aspects of fluxon motion will be described in detail for two specific sets of parameters. These two sets were chosen because they are encountered in most types of periodic and nonperiodic motions found in our simulations. Calculations presented here were carried out with a time span at $\Delta t = 0.025$ and a length span of $\Delta x = 0.05$. For periodic solutions calculations were continued until good periodic wave forms of $\phi_x(0,t)$ were achieved. Usually times of $t \leq 2000$ were needed. For nonperiodic solutions, a long period of $t = 4000$ was used to be certain that the solutions were really nonperiodic.

A. *I-V* curve

In an external magnetic field fluxon propagation in a junction leads to a set of current steps in the *I-V* curve of a long Josephson junction. In our computation such a curve corresponds to the v versus $\langle \phi_t(0,t) \rangle$ behavior. Figure 2 shows this behavior computed using Eq. (1) for the conditions of $\alpha = 0.26$, $\beta = 0.0$, $\eta = 1.25$, and $L = 5$. Three Fiske steps are shown. The dots are the computed points and the line is a guide for the eye. In Figs. 3(a), 3(b), and 3(c) we show the evolutions of $\phi_x(x,t)$ for the periodic solutions at the steps FS1, FS2, and FS3, respectively. The physical meaning of FS1 corresponds to the situation where a fluxon propagates in the bias current-aided direction and it is reflected at $x = 0$ as a localized plasma wave. This plasma wave moves in the opposite direction and it is reflected at $x = L$ as a fluxon. The physical meaning of FS3 is not simple, as it can maintain different modes; one mode shown in Fig. 3(c) corresponds to the case of two fluxons and a plasma wave moving in opposite directions at the same time. After a reflection it becomes two plasma waves and one fluxon, and so on. FS2 is also complicated as it can have a few modes. In this situation, according to Fig. 3(b) one mode corresponds at first to two fluxons moving together and then changing to a fluxon and a plasma wave moving in opposite directions at the same time. When they hit the junction boundaries a set of plasma waves is produced. After moving for a while, two successive fluxons are produced again and they then move in the bias current-aided direction. The system then continues in this sequence repeating the process just described. The average voltage $\langle \phi_t \rangle$ in the situation shown in Fig. 3(b) is compared with $\langle \phi_t \rangle$ for a simple FS2 which will be discussed in subsection D. Both $\langle \phi_t \rangle$ have similar values as they belong to FS2.

It is important to note that periodic oscillations at FS1 and FS2 in Fig. 2 occupy only a small portion of the Fiske steps in the v versus $\langle \phi_t \rangle$ curve. Most of the parts are chaotic; this type of motion will be discussed in the remaining parts of this section.

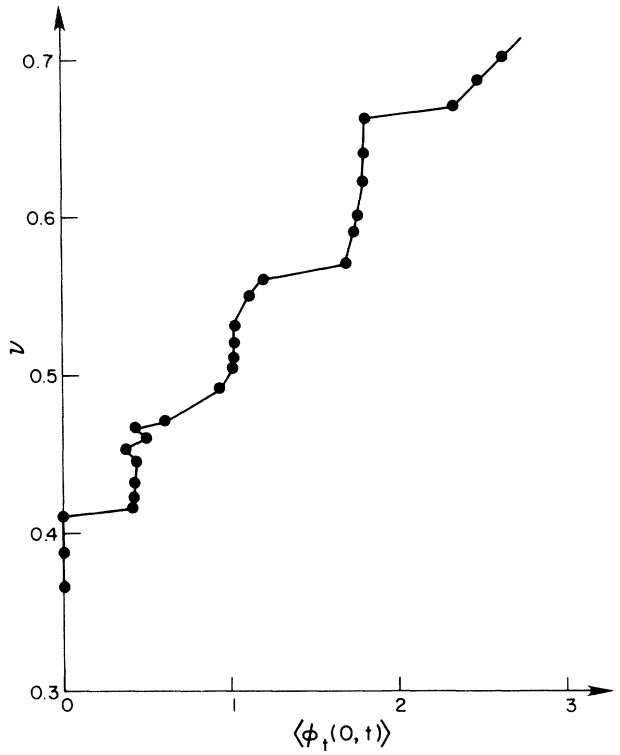

FIG. 2. The v vs $\langle \phi_t(0,t) \rangle$ curve calculated under the condition of $\alpha = 0.26$, $\beta = 0$, $\eta = 1.25$.

B. Period-doubling bifurcations

The details of period-doubling bifurcations in our system have been published elsewhere.[18] For the sake of completeness a brief description will be given here. Careful examination of how the system changes from periodic motion to nonperiodic at FS1 in Fig. 2 leads to the following observations. For a narrow range of v values ($v = 0.417 - 0.429$) the solutions are stable and the fundamental frequency is equal to the Josephson frequency. At $v = 0.430$ the system starts to bifurcate. As v is further increased, the system goes through period-2, period-4, and period-8 bifurcations. At $v = 0.436$ the $f/8$ peaks have "skirts" of broadband noise and at $v = 0.44$ the system is in the fully developed chaotic regime. When $v = 0.455$ is reached, there is a period-3 window (it is always present in one-dimensional quadratic iteration maps). Figure 4 shows the power spectra for the situations of period 1, noisy period 8, and chaos. A further increase in v causes the system to switch into another periodic mode of the FS1 with a subsequent chaotic regime which is reached through another cascade of period-doubling bifurcation sequences.

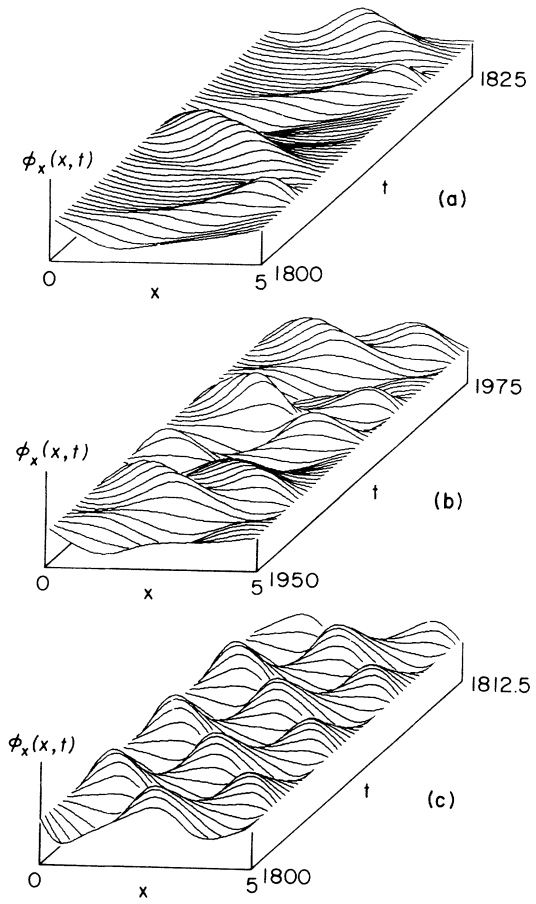

FIG. 3. Evolutions of $\phi_x(x,t)$, obtained at (a) FS1, $\nu=0.42$; (b) FS2, $\nu=0.51$; and (c) FS3, $\nu=0.60$. Other parameters are the same as those in Fig. 2.

These results clearly demonstrate the existence of temporal chaotic regimes. The cascade of period-doubling bifurcations can be modeled by a one-dimensional iteration map. This indicates that a high-dimensional system such as ours can be considered in a low-dimensional strange attractor for certain ranges of parameters.

C. Intermittent chaos

Intermittent chaos was often encountered in our simulations. Some of it occurred between Fiske steps while others appeared within the steps. For the case shown in Fig. 2, as ν is increased from 0.465 the system enters an intermittent chaotic region where the system jumps back and forth between FS1 and FS2. From the wave form shown in Fig. 5(a), the front part resembles the wave at FS1 while the end part is similar to the FS2 case. The intermittent chaotic region ranges from $\nu=0.465$ to 0.505. The values of $\langle \phi_t(0,t) \rangle$ increase from 0.6 to 1.0. Our results are similar to those obtained by Sorenson *et al.*[15] In real experiments this type of chaos can be easily identified as it corresponds to large amounts of noise in the regions between Fiske steps where the dynamic resistance has finite positive values.

Fluxons which are in the junction have to move in one of the resonances that the system allows, FS1 or FS2. When the number of fluxons produced by the magnetic field and bias current is larger than can be accommodated at FS1 and less than the number needed for FS2, this causes an instability which leads to the intermittent chaos.

For a small range of ν (0.505–0.51) the system is in the periodic FS2 mode as shown in Fig. 3(b). Above $\nu=0.51$, the system loses periodicity. At first the fluxon motion resembles the pattern of that FS2 mode and then it changes to a different FS2 mode, which corresponds to a fluxon and a plasma wave moving in opposite directions at the same time. As ν is further increased, the motion becomes fully chaotic. Any part of the motion can be recognized as one of the FS2 modes mentioned above. In this sense, the chaotic motion can be viewed as intermittent chaos. Figure 5(b) shows the wave pattern and power spectrum in this region. Because this intermittency consists of switching between two kinds of FS2 modes, the system remains in the chaotic FS2 mode until $\nu=0.57$ is reached. This is a typical example illustrating that intermittent chaotic motion originates from the interaction between two different modes within one Fiske step.

D. Quasiperiodicity

As ν reaches 0.57, the system switches to the FS3. At the beginning of this step, the motion shows quasiperiodic behavior with modulation in both the amplitude and frequency. When ν is increased further, such modulation becomes smaller, and at $\nu=0.58$ the motion becomes fully periodic. Figure 6(a) shows the wave form and power

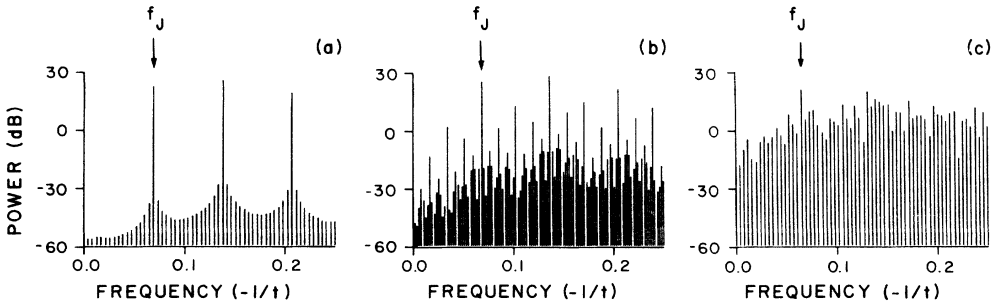

FIG. 4. Power spectra of $\phi_t(0,t)$ in the period-doubling bifurcation regime. (a) Period 1, $\nu=0.422$; (b) noisy period 8, $\nu=0.436$; and (c) chaos, $\nu=0.44$. Other parameters are the same as those in Fig. 2.

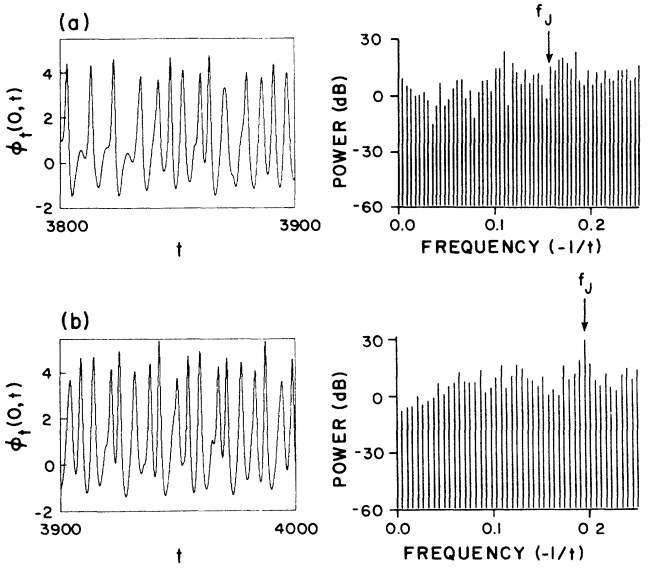

FIG. 5. Wave forms and power spectra of $\phi_t(0,t)$ in intermittent chaotic regimes. (a) Between FS1 and FS2, $\nu=0.49$. (b) Within FS2, $\nu=0.54$. Other parameters are the same as those in Fig. 2.

spectrum at the quasiperiodic region. As a comparison, Fig. 6(b) shows the wave form and power spectrum at the fully periodic FS3.

Another interesting phenomenon found in the simulation is an instability which occurs at the center of a Fiske step. One set of parameters for this case is $\alpha=0.30$, $\beta=0.0$, $\eta=1.4$. For these conditions when ν is in the range of 0.363–0.47 the system is in the periodic regime of FS1; then in enters a weak chaotic regime in a narrow

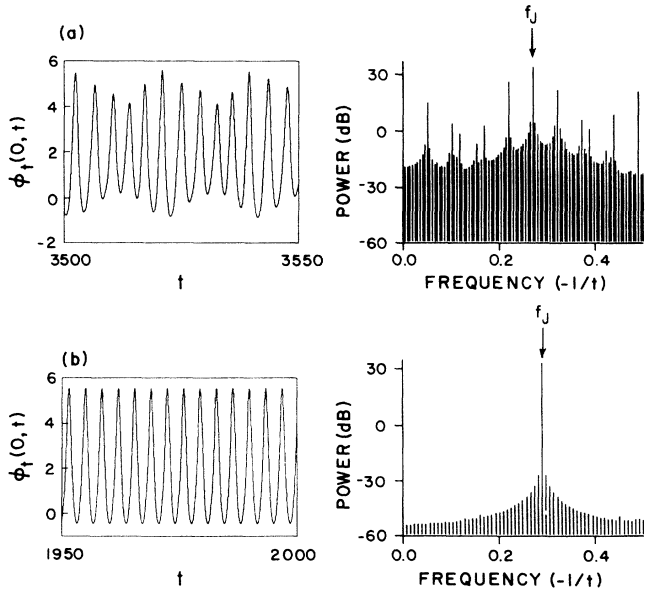

FIG. 6. Wave forms and power spectra of $\phi_t(0,t)$ obtained at FS3. (a) At the quasiperiodic regime, $\nu=0.562$. (b) At the fully periodic regime $\nu=0.60$. Other parameters are the same as those in Fig. 2.

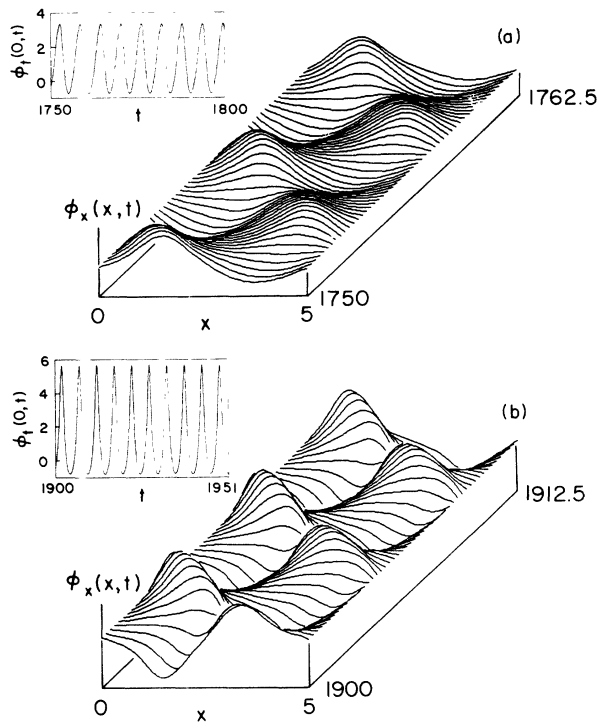

FIG. 7. Evolutions of $\phi_x(x,t)$ and wave forms of $\phi_t(0,t)$ obtained at (a) first FS2, $\nu=0.49$; (b) second FS2, $\nu=0.69$. Other parameters are $\alpha=0.30$, $\beta=0$, $\eta=1.4$.

range of ν. At $\nu=0.49$ the system enters a good periodic regime for FS2; for this situation the evolution of $\phi_x(x,t)$ and the wave form of $\phi_t(0,t)$ are presented in Fig. 7(a). Physically this mode of FS2 corresponds to a fluxon and a plasma wave moving in opposite directions at the same time. When ν is above 0.51 the motion becomes nonperiodic as demonstrated by the time variation of the amplitudes of the peaks in the plot of $\phi_t - t$. As ν is increased further, the difference between the highest and lowest peaks reaches a maximum at $\nu=0.61$. Figure 8(a) shows the wave form of ϕ_t for that moment. Beyond $\nu=0.61$ the difference becomes smaller. Eventually at $\nu=0.70$ the system enters another periodic FS2 mode

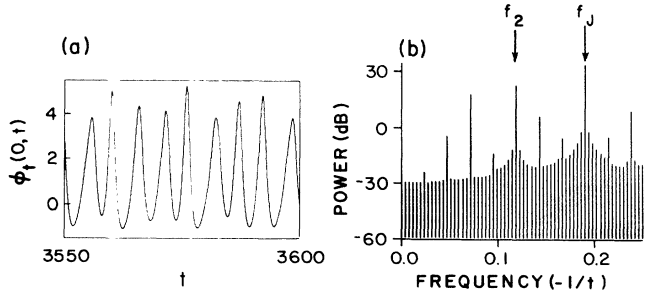

FIG. 8. The wave form and power spectrum of $\phi_t(0,t)$ obtained in the quasiperiodic region, $\nu=0.61$. Other parameters are the same as those in Fig. 7.

where the evolution of $\phi_x(x,t)$ and the wave form of $\phi_t(0,t)$ are shown in Fig. 7(b). The physical interpretation of this FS2 mode is similar to the one in Fig. 7(a), the only difference being that the amplitudes of the plasma wave and the fluxon are larger for the latter FS2 mode.

The special feature of this nonperiodic motion is that the system in this range is not chaotic. Figure 8(b) shows the power spectrum taken at $\nu=0.61$. It shows the Josephson frequency and another distinct peak marked f_2 in Fig. 8(b). Other peaks appearing in the spectrum come from sidebands of these two frequencies. This quasiperiodic motion comes from two competing frequencies. From the wave form in Fig. 8(a) it can be seen that some of the peaks which have small amplitude with a wide width are similar to the ones in the first FS2 mode shown in Fig. 7(a), while others are analogous to those in the second FS2 mode shown in Fig. 7(b). The system moves back and forth between the two FS2 modes. Since the two FS2 modes are similar, the system is driven only into quasiperiodic motion. Although the noise level in this situation is higher than in the periodic case, it is still lower than in the real chaotic spectrum (Fig. 5).

V. OCCURRENCE OF CHAOS

Following the preceding sections where we showed the various types of nonperiodic behavior found in our simulations, we present results on the search for chaotic motion in our system with $\beta=0$, $L=5$, and one fluxon as initial conditions. In the survey for a specific set of parameters, ν is increased from a small value with a relatively large span until the flux-flow state is reached. For each point the conditions used are $\Delta t=0.05$, $\Delta x=0.1$, and the total $t=600$. The time interval of 600 is usually long enough for periodic solutions to reach a stable state. For each chaotic region a few selected points were checked by running longer to confirm the existence of chaos.

Figure 9 shows the calculated periodic and chaotic regions in the α-η plane. In the periodic regime, the behavior shows no chaos for the whole I-V (ν versus $\langle\phi_t\rangle$) curve. The shaded area corresponds to chaos in certain sections of the I-V curve, while others may not be chaotic in that regime. Although Fig. 9 shows the boundary between periodic and chaotic regimes, this boundary is really quite broad and diffuse; the chaotic regime gradually disappears when this boundary is crossed.

In preceding sections we have examined the chaotic behavior for $\alpha=0.26$ and $\eta=1.25$. For that situation chaos occurred mainly within FS1 and FS2. When α is decreased, the widths of the steps FS1 and FS2 shrink and the chaotic region is pushed towards the beginning of the I-V curve. Figure 10 shows the I-V curve for $\alpha=0.2$ and $\eta=1.25$; the chaotic and periodic regions are marked. In the range of ν from 0.40 to 0.47, an up and down computation was made with ν first increasing to 0.47 and then decreasing to 0.40. Hysteresis is clearly observed, and this is shown in Fig. 10. When ν is increased from zero, the system enters a chaotic regime as soon as a voltage appears ($\nu=0.43$). According to the calculated value of $\langle\phi_t\rangle$ the system is in a FS2. The inset of Fig. 10 shows the wave form of ϕ_t in the chaotic regime. As ν is increased to 0.447, the system switches into the periodic FS3. The chaotic regime extends from $\nu=0.43$ to 0.447.

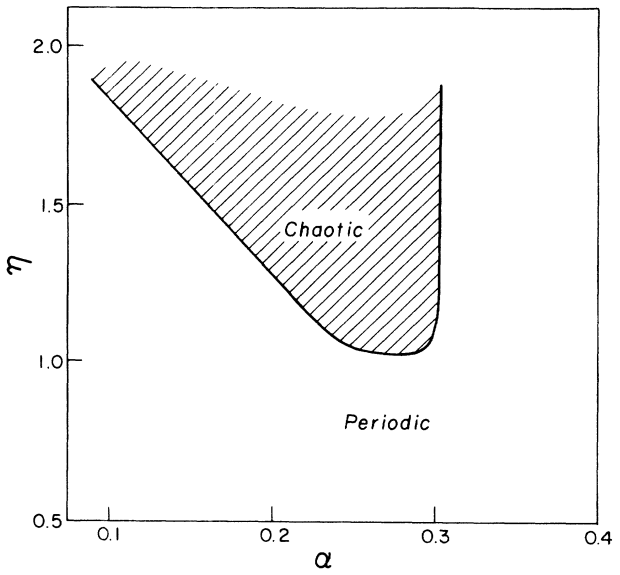

FIG. 9. Boundary between chaotic and periodic regimes in the η-α plane.

Let us consider now the boundary between periodic and chaotic regimes in the α-η plane. In the low-α range, the general I-V curves and wave forms are similar to the ones just discussed above. But as α decreases while η is kept unchanged, the chaotic range ΔC [$=\nu_h$ (higher boundary of the chaotic range in the I-V curve) $-\nu_l$ (lower boundary of the chaotic range also in that curve)] shrinks. For example, when $\eta=1.25$, ΔC is 0.05 for $\alpha=0.22$, and it reduces to 0.017 for $\alpha=0.2$; it almost disappears for $\alpha=0.17$. When η is increased while α is kept constant, the chaotic range in the I-V curve in-

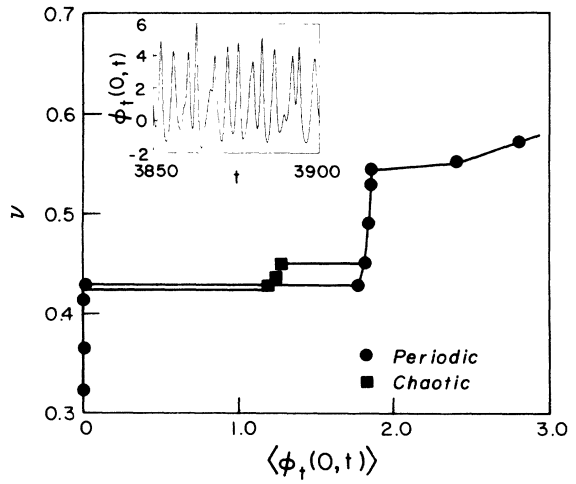

FIG. 10. The ν vs $\langle\phi_t(0,t)\rangle$ curve obtained at $\alpha=0.2$, $\beta=0$, and $\eta=1.25$. The inset is the wave form of $\phi_t(0,t)$ obtained in the chaotic regime, $\nu=0.44$.

creases. For instance, when η is increased from 1.25 to 1.4 for $\alpha=0.2$, ΔC expands from 0.017 to 0.08. The competition between α and η in the low-α range causes the gently slanted boundary of the chaotic regime extended from $\alpha=0.2$, $\eta=1.25$ to $\alpha=0.1$, $\eta=2.0$ (this is the highest value we have calculated for η). It is believed that if η is increased further, the chaotic regime could extend to smaller values of α.

Now let us examine the boundary in the high-α range. For $\alpha>0.25$, the general pattern of the I-V curve is similar to that of $\alpha=0.26$, $\eta=1.25$. Usually three steps (FS1, FS2, FS3) and sometimes two steps (FS1, FS2) are found for each specific set of parameters. As α increases beyond 0.26, the chaotic range in the I-V curve also shrinks. For $\alpha=0.3$, $\eta=1.4$, besides the quasiperiodic motion already described, the real chaos only happens between FS1 and FS2 and ΔC is merely 0.01. When α is increased to 0.35, the chaotic motion disappears. In the high-α range in contrast with the low-α range, the increase of η does not cause an expansion of the chaotic range in the I-V curve. So it is safe to draw a straight line at 0.3 as a higher boundary of the chaotic regime in the α-η plane. Finally, it is important to note that chaotic behavior was not found for η less then 1.

VI. THE INFLUENCE OF β ON CHAOTIC MOTIONS

For simplicity, $\beta=0$ was chosen for our calculations. In real situations, the β term represents an important dissipation mechanism for the motion of fluxons. In order to obtain an idea of how the chaotic behavior is influenced by β, for two cases ($\alpha=0.26$, $\eta=1.25$, and $\alpha=0.2$, $\eta=1.25$) which have been calculated in detail without β, recalculations are performed with β.

For the case of $\alpha=0.26$, $\eta=1.25$, $\beta=0.01$, in a small range of ν (0.437–0.44) a stable period 1 of FS1 is established. After ν exceeds 0.44, the system bifurcates to a period-2 mode of FS1. At $\nu=0.442$, the system suddenly enters the chaotic region. The cascade of period-doubling bifurcation observed in the situation without β is now truncated by the chaotic region. As ν is increased further, intermittent switching between FS1 and FS2 is observed, and then at $\nu=0.48$, the chaotic FS2 mode is entered. At the beginning part of FS2, the wave form is similar to the stable FS2 shown in Fig. 3(b), but is not exactly periodic. The system stays in the chaotic FS2 region for a while and switches to the periodic FS3 which is the same as the situation shown in Fig. 3(c). Finally the system enters the flux-flow state at $\nu=0.60$. In comparison with the situation without β, the major changes for $\beta=0.01$ are that the periodic FS2 behavior which existed for $\beta=0$ disappears. As for the chaotic motion, the basic chaotic behaviors observed without β are found here.

Now we will discuss the results of calculations with $\beta=0.05$. In the case of $\alpha=0.26$, $\eta=1.25$, $\beta=0.05$, the system is in a good periodic FS1 state from $\nu=0.45$ to 0.48. After ν exceeds 0.48, a weak chaos develops in a small range of ν and then the system switches into quasiperiodic FS2. The system remains in the state of quasiperiodic FS2 for a while and then gradually enters a periodic FS2 state whose wave form is similar to that shown in Fig. 7(b). When ν is beyond 0.7, the system enters the flux-flow state. The two features, the chaotic motion shrinking to a very small range and the quasiperiodic motion developing in FS2, are quite similar to those found in the case of $\alpha=0.3$, $\eta=1.4$, and $\beta=0$.

For the case of $\alpha=0.2$, $\eta=1.25$, $\beta=0.05$, the I-V curve and wave forms are similar to the ones without β which have been described in detail in Sec. V. The only difference is that the chaotic range ΔC in the I-V curve is increased from 0.017 for $\beta=0$ to 0.036 for $\beta=0.05$. The result of $\Delta C=0.036$ is comparable with $\Delta C=0.05$ obtained in the case of $\alpha=0.22$, $\eta 1.25$, $\beta=0$.

The main conclusion drawn from the above results are that as far as the chaotic behavior is concerned, there is not much change when a small β is included in the equation; for relatively large β, the chaotic motion with β term resembles that having a larger α term with $\beta=0$.

VII. DISCUSSION

We have demonstrated that various chaotic behaviors can occur in long Josephson junctions with dc current bias in the presence of external magnetic fields. The chaos routes from a cascade of period-doubling bifurcations is found in two places. Several intermittency chaotic motions, including switching between two FS states and between two different modes in one FS are observed in the simulation. Two kinds of quasiperiodicity have been found; one in the beginning of FS3 with amplitude and frequency modulation and another one in the center of one FS. A physical explanation for the occurrence of chaos in our system is provided, and it can explain most of our observations. From an experimental point of view, our findings can be summarized as follows: Chaos can occur between two adjacent FS's as shown in Fig. 5(a), in parts next to a FS as discussed in Sec. IV B and IV C, or within a whole FS as shown in Fig. 10. Nonperiodic motion also can occur at the beginning of FS3. Indeed, all these findings were observed in experiments.[15,17]

The hysteresis between FS's as shown in Fig. 10 is a common phenomenon. The widths of the hysteresis $\Delta\nu$ between zero and FS2 and between FS2 and FS3 in Fig. 10 are 0.004 and 0.01, respectively. They are very narrow, and any thermal noise could reduce the width further. If the system is biased within the hysteresis region, external noise such as thermal noise, current fluctuations in the current source, or the chaotic motion inside the junction may cause the system to jump back and forth between two FS's in a low-frequency fashion. Actually, it may even be responsible for the low-frequency telegraph noise observed in experiments.[17,23]

We have done a survey of chaotic regions for specific conditions. The result shows that chaos can occur for $\alpha\leq 0.3$, which is a very common range for long Josephson junctions. The chaotic behavior has to be taken into consideration when applications of long Josephson junctions are planned, especially for parameters in the range discussed here. It is also necessary to mention that the chaotic motion in our system has been only examined in a

small portion of the parameter manifold. The change of some parameters, for example, length L or initial conditions, may give rise to different kinds of chaotic behavior or even more complicated phenomena.

ACKNOWLEDGMENTS

This work was supported by Air Force Grant No. AFOSR-86-0020.

*Present address: Department of Physics, University of Idaho, Moscow, ID 83843.

[1]A. C. Scott, Nuovo Cimento B **69**, 241 (1970).

[2]R. D. Parmentier, in *Solitons in Action,* edited by K. Lonngren and A. C. Scott (Academic, New York, 1978), p. 173.

[3]N. F. Pederson, in *Advances in Superconductivity,* edited by B. Deaver and Jahn Ruvalds (Plenum, New York, 1982), p. 149.

[4]A. Barone and G. Paterno, *Physics and Applications of the Josephson Effect* (Wiley-Interscience, New York, 1982).

[5]K. K. Likharev, *Dynamics of Josephson Junctions and Circuits* (Gordon and Breach, Amsterdam, 1986).

[6]A. C. Scott, Flora Y. F. Chu, and Stanley A. Reible, J. Appl. Phys. **47**, 3272 (1976).

[7]A. Matsuda and T. Kawakami, Phys. Rev. Lett. **51**, 694 (1983).

[8]A. R. Bishop and P. S. Lomdahl, Physica **18D**, 54 (1986).

[9]A. R. Bishop, K. Fesser, P. S. Lomdahl, W. C. Kerr, M. B. Williams, and S. E. Trullinger, Phys. Rev. Lett. **50**, 1095 (1983).

[10]K. Nozaki, Phys. Rev. Lett. **49**, 1883 (1982).

[11]L. E. Guerrero and M. Octavio, in Proceedings of the 18th International Conference on Low Temperature Physics, LT-18, Kyoto, 1987, edited by Y. Nagaoka [Jpn. J. Appl. Phys. **26**, 1641 (1987)], Suppl. 26-3.

[12]T. A. Fulton, R. C. Dynes, and P. W. Anderson, Proc. IEEE **61**, 28 (1973).

[13]D. P. McGinnis, G. K. G. Hohenwarter, M. Ketkar, J. B. Beyer, and J. E. Nordman, IEEE Trans. Magn. MAG-25, 1258 (1989).

[14]K. Yoshida, T. Hashimoto, K. Enpuku, and K. Yamafuji, in Proceedings of the 18th International Conference on Low Temperature Physics, LT-18, Ref. 11, p. 1582.

[15]M. P. Soerenson, N. Arley, P. L. Christiansen, R. D. Parmentier, and O. Skovgaard, Phys. Rev. Lett. **51**, 1919 (1983).

[16]M. Cirillo, G. Costabile, S. Pace, R. D. Parmentier, and B. Save, in *Proceedings of the 17th International Conference on Low Temperature Physics, LT-17,* edited by U. Ekern, A. Schmid, W. Weber, and H. Wühl (North-Holland, Amsterdam, 1984), p. 1131.

[17]B. S. Han, B. Lee, O. G. Symko, W. J. Yeh, and D. J. Zheng, IEEE Trans. Magn. **MAG-25**, 1396 (1989).

[18]D. J. Zheng, W. J. Yeh, and O. G. Symko, Phys. Lett. A **140**, 225 (1989).

[19]J. C. Eilbeck, P. S. Lomdahl, O. H. Olsen, and M. R. Samuelsen, J. Appl. Phys. **57**, 861 (1985).

[20]P. S. Lomdahl, O. H. Soerensen, and P. L. Christiansen, Phys. Rev. B **25**, 5737 (1982).

[21]A. R. Bishop, K. Fesser, P. S. Lomdahl, and S. E. Trullinger, Physica **7D**, 259 (1983).

[22]O. H. Olsen and M. R. Samuelsen, J. Appl. Phys. **52**, 6247 (1981).

[23]B. S. Han, B. Lee, O. G. Symko, and D. J. Zheng, in Proceedings of the 18th International Conference on Low Temperature Physics, LT-18, Ref. 11, p. 1551.